Published in final edited form as:
Mol Pharm. 2014 February 3; 11(2): 545–559. doi:10.1021/mp4005035.

Modulation of pyridinium cationic lipid-DNA complex properties by pyridinium gemini surfactants and its impact on lipoplex transfection properties

Vishnu Dutt Sharma[1], **Julia Lees**[1], **Nicholas E. Hoffman**[2], **Eugen Brailoiu**[2], **Muniswamy Madesh**[2], **Stephanie L. Wunder**[3], and **Marc A. Ilies**[1,*]

[1]Department of Pharmaceutical Sciences and Moulder Center for Drug Discovery Research, Temple University School of Pharmacy, 3307 N Broad Street, Philadelphia, PA-19140

[2]Temple University, School of Medicine, Center for Translational Medicine, 3500 N. Broad Street, Philadelphia, PA-19140

[3]Temple University, College of Science and Technology, Department of Chemistry, 130 Beury Hall, 1901 N. 13th Street, Philadelphia, PA-19122

Abstract

The study presents the effects of blending a cationic gemini surfactant into cationic lipid bilayers and its impact towards plasmid DNA compaction and delivery process. Using nanoDSC, dynamic light scattering, zeta potential and electrophoretic mobility measurements, together with transfection (2D- and 3D-) and viability assays, we identified the main physicochemical parameters of the lipid bilayers, liposomes and lipoplexes that are affected by the gemini surfactant addition. We also correlated the cationic bilayer composition with the dynamics of the DNA compaction process, and with transfection efficiency, cytotoxicity and internalization mechanism of the resultant nucleic acid complexes. We found that blending of gemini surfactant into the cationic bilayers fluidized the supramolecular assemblies, reduced the amount of positive charge required to fully compact the plasmid DNA and, in certain cases, changed the internalization mechanism of the lipoplexes. Transfection efficiency of select ternary lipoplexes derived from cationic gemini surfactants and lipids was several times superior to transfection efficiency of corresponding binary lipoplexes, also surpassing standard transfection systems. The overall impact of gemini surfactants into the formation and dynamic of cationic bilayers was found to depend heavily on the presence of co-lipids, their nature and amount present into lipoplexes. The study confirmed the possibility of combining the specific properties of pyridinium gemini surfactants and cationic lipids synergistically for obtaining efficient synthetic transfection systems with negligible cytotoxicity useful for therapeutic gene delivery.

Keywords

transfection; gemini surfactant; cationic lipid; synergy; lipoplex; pyridinium

*To whom correspondence should be addressed: Dr. Marc A. Ilies, Department of Pharmaceutical Sciences, Temple University School of Pharmacy, 3307 N Broad Street, Philadelphia, PA-19140, Tel 215-707-1749, Fax 215-707-5620, mailies@temple.edu.

Introduction

Gene therapy has the potential to be a widespread cure for diseases caused by hereditary or acquired genetic defects, treating the source of the disease rather than its symptoms. It relies on the transfer and expression (transfection) of foreign genetic material into affected cells of a patient, either to correct a defective gene or to introduce a new function to the targeted cells. Within this new therapy, DNA, small interfering RNA (siRNA) and other nucleic acids are used as "drugs", but even more important than the drug itself becomes its efficient and selective delivery to the target cells and the side effects associated with the delivery process.[1–3] Thus, viruses are very efficient gene delivery vectors but their use is associated with immunogenicity, mutagenicity and safety concerns that make their repeated administration problematic. A top-down approach is currently underway attempting to delete or replace the immunogenic structural elements.[2] In contrast, chemical methods relying on the use of self-assembled systems designed bottom up are safer and allow the delivery of DNA plasmids of practically unlimited size.[4] However, their efficiency is relatively low due to an incomplete adaptation of the structure of the synthetic delivery system to the transfection barriers in vitro and in vivo.[5,6]

Synthetic transfection systems rely on the use of cationic amphiphiles (surfactants,[7,8] gemini-,[9–12] trimeric- and oligomeric surfactants,[13] lipids,[14,15] dendrons, dendrimers and polymers[16]) with different sizes, shapes, and self-assembling properties. Small MW cationic amphiphiles cooperatively associate and compact nucleic acids through a major structural rearrangement process entropically-driven by the release of counterions and hydration water of both species. Safinya's group revealed the existence of lamellar (L_α^C)[17] and inverted hexagonal (H_{II}^C)[18] structures for the lipoplexes, with the later one being more transfection-efficient than the first one. The preferential formation of one of these structures depends on the overall packing parameter of the amphiphile (or mixture of amphiphiles) used to compact the DNA.[19–21] Since most of cationic lipids have packing parameters lower than 1, co-lipids with $P > 1$ such as DOPE or cholesterol (Chol, C) are blended with cationic lipids in order to induce an average packing parameter around 1 (and thus generate a lamellar structure for the lipoplex) or over 1 (when the inverted hexagonal structure is obtained, usually requiring a larger amount of colipid). The co-lipid also reduces the electrostatic repulsions between adjacent cationic polar heads and ensures the robustness of the lipoplex through the strong hydrophobic effect that keeps the individual amphiphiles together. The ability of lipoplexes to resist the disruptive interaction with serum proteins and figurative elements of the blood is essential for the success of nucleic acid delivery via IV administration route. Once the target tissue is reached, the lipoplexes interact with the cells via multiple mechanisms (clathrin, caveolin, endocytosis/pinocytosis), being internalized and ending into internal vesicles of various structures and dynamics (clathrin coated pits, caveolae, endosomes). Once inside the cell, the supramolecular delivery system must be able to rupture the internal vesicle, disassemble fast and release its nucleic acid cargo into the cytoplasm, from where it can relocate to the nucleus and be internalized, transcribed and later translated into encoding proteins. For lipoplexes internalized via endocytosis/pinocytosis Safinya's group revealed that endosomal escape is favored by a high charge density of the lipoplex and a high elastic modulus of the lipoplex membrane-forming

amphiphiles.[22] Other studies emphasized the importance of co-lipid used in liposome and lipoplex formulation, showing the stabilizing effect of cholesterol on the lipoplex transfection efficiency even at high cationic lipid/DNA charge ratios and in the presence of large amounts of serum.[23,24]

It is thus obvious that for efficient nucleic acid delivery the cationic lipid mixture must be able to accommodate both processes of DNA compaction and release. Cationic amphiphiles with a soft cationic charge are particularly suited for accommodating these antagonistic processes. They also display a reduced interaction with serum proteins which makes them well suited for in vivo use.[25,26] The softer charge can be generated through the use of large positively charged atoms (e.g. phosphonium, arsonium instead of ammonium[26–28]) or through the use of heterocyclic systems where the positive charge is delocalized on several atoms. Among the heterocyclic representatives the imidazolium[29] and pyridinium cationic lipids have proven their efficiency both in vitro and in vivo for the delivery of DNA and siRNA.[7,13,30–34] Our team successfully generated pyridinium amphiphiles through the reaction of pyrylium salts with primary amines under Bayer-Piccard reaction conditions.[13,32,33] The procedure is versatile and allows the access to pyridinium lipids, surfactants, gemini surfactants, and oligomeric amphiphiles.[13] Extensive structure-activity relationship (SAR) studies conducted in recent years allowed us to identify efficient members within each class of above-mentioned pyridinium amphiphiles, such as lipids SPYRIT-7[33] and gemini surfactants SPYRIT-35 and SPYRIT-68[7,13,33,35,36] (Chart 1), together with their most efficient formulations.

Thus, cationic lipid SPYRIT-7 co-formulated with cholesterol at 1:1 molar ratio proved efficient in transfecting reported gene plasmids in several malignant cell lines while displaying negligible cytotoxicity.[33] An even better transfection profile was displayed by gemini surfactant SPYRIT-68, evolved throughout our synthetic program and SAR studies within this class of amphiphiles.[36] Importantly, lipoplexes based on SPYRIT-68/DOPE (1/2 molar ratio) formulation were able to retain their transfection efficiency even in the presence of elevated levels of serum in the transfection media, mimicking the in vivo conditions.[36] However, the cytotoxicity of these lipoplexes was higher, probably due to the efficient membrane destabilitation properties of this class of amphiphiles, which is related with their higher charge/mass ratio, higher curvature and molecular flexibility and lower packing parameter as compared with their lipid congeners.[9, 36] Therefore we decided to investigate the use of gemini surfactant SPYRIT-68 in mixture with pyridinium lipid SPYRIT-7 seeking to combine the membrane-destabilization properties of the gemini surfactant, its high charge/mass ratio and its excellent transfection properties with the good transfection/ cytotoxic profile of SPYRIT-7 based formulations. The cationic gemini surfactant/lipid blends were expected to have a higher charge density than corresponding pure cationic lipid-based formulations, while displaying reduced cytotoxicity, thus synergistically combining the properties of the two classes of cationic amphiphiles for overcoming some of the intracellular delivery barriers (such as endosomal escape) against gene delivery.

Materials and methods

Materials

The pyridinium cationic lipid SPYRIT-7, and the gemini surfactant SPYRIT-68 were synthesized and purified as previously reported.[33,35,36] Cholesterol, DOTAP, DOPE were from Avanti Polar Lipids (Alabaster, AL) and were used as received. Solvents (HPLC quality) were from Fisher Scientific (Pittsburgh, PA), EMD (Gibbstown, NJ), and VWR International (West Chester, PA). Chloropromazine hydrochloride, genistein and EIPA were from Enzo Life Sciences (Farmingdale, NY). Tris Acetate EDTA (TAE) buffer, Lambda DNA/*Hin*d III markers, Blue juice – Blue/Orange Loading dye were from Promega (Madison, WI). DNA plasmids - gWiz™ Luc plasmid encoding the firefly luciferase gene and gWiz™ GFP encoding the green fluorescent protein were from Aldevron (Fargo, ND). The GelStar Nucleic acid gel stain was from Lonza (Rockland, ME). Agarose (ultrapure) and Optimem media were from Invitrogen (Carlsbad, CA).

Methods

Preparation of hydrated lipid bilayers—Stock solutions (3 mM) of the cationic lipid SPYRIT-7 and of gemini surfactant SPYRIT-68 (0.3 mM) were prepared from powder in glass vials using $CHCl_3$/MeOH (2/1) as solvent (organic stock). For DOPE and cholesterol, solutions of the same concentration (3 mM) were made in $CHCl_3$/MeOH (2/1) as well. All solutions were swirled, purged with nitrogen, and capped securely; when not in use they were stored in the freezer at −20 °C.

Thirteen preparations were done, namely cationic lipid alone, cationic lipid mixed with cholesterol at 1:1 and 1:2 molar ratio, cationic lipid mixed with DOPE at 1:1 and 1:2 molar ratio, cationic lipid/gemini surfactant (95/2.5 molar ratio) with cholesterol at 1:1 and 1:2 molar ratio, and cationic lipid/gemini surfactant (95/2.5 molar ratio) with DOPE at 1:1 and 1:2 molar ratio, cationic lipid/gemini surfactant (90/5 molar ratio) with cholesterol at 1:1 and 1:2 molar ratio, and cationic lipid/gemini surfactant (90/5 molar ratio) with DOPE at 1:1 and 1:2 molar ratio. Thus 20 μL of the SPYRIT-7 organic stock (3 mM) was transferred into a glass vial (total cationic lipid was 60 nmol). An amount of 20 or 40 μL cholesterol or DOPE organic stock (3mM) was added to the vial for formulations containing colipids. In the case of gemini surfactant blends, 18 or 19 μL of SPYRIT-7 cationic lipid organic stock (3 mM) were combined with either 10 or 5 μL of SPYRIT-68 gemini surfactant organic stock (0.3 mM) and 20 or 40 μL of cholesterol or DOPE (3 mM stock) respectively. Each sample was diluted with $CHCl_3$/MeOH (2/1) to a final volume of 500 μL. The organic solvent was evaporated to dryness in the SpeedVac for 1 h, and then the samples were further dried under vacuum in a dessicator for another hour. The dry lipid films were hydrated with 0.6 mL of deionised water yielding a 0.1 mM positive charge-containing suspension. The vials were purged with sterile nitrogen passed through a 0.22 μm filter, sonicated at room temperature for 1 min, and then left overnight at room temperature to hydrate.

The next day, each vial was freeze-thawed 10 times (−70°C/65°C).

Nano-differential scanning calorimetry—For the nanoDSC experiments the same protocol was followed except specified amounts of organic stock aliquoted out were amplified 33.3X and the lipid films were hydrated with 1 mL deionized water. DSC measurements of the hydrates samples were obtained on a TA Instruments (New Castle, DE) NanoDSC-6300, between 5 and 95 °C, using a heating/cooling rate of 1 °C/min on 0.75 mL sample (working cell volume). No other transition temperatures except the ones represented in Figure 1 were observed. Experimental data was worked out using CpCalc software version 2.2 (Calorimetry Sciences Corp).

Liposome Preparation—The hydrated samples (0.1 mM total positive charge) prepared as described above were subsequently sonicated twice for 15 minutes at 65°C with a 15 minute pause between cycles yielding homogeneous liposomal formulations.

Liposome Characterization: A volume of 500 μL of each liposomal preparation was introduced into a disposable Malvern DTS 1060 measurement cell. The size and zeta potential of the liposomes were measured using a Zetasizer Nano (Malvern Instruments). The readings were all made at 25°C at normal resolution, using the instrument's automated feature. For the size measurements, the volume results were used in all cases, and the results were reported as the average of 10–20 runs. Zeta potentials were measured in millivolts (mV) and were the average of 10–20 runs.

Lipoplex preparation and characterization: Solutions of plasmid DNA (gWiz™ Luc plasmid, Aldevron, 6732 bp), and ladder Lambda DNA/*Hin*d III (Promega), both 0.05 μg/μL, were prepared in sterile conditions, using nuclease-free water.

In six eppendorff tubes, 5 μL of diluted DNA stock were treated with 8 μL, 16 μL, 24 μL, 32 μL, 40 μL, and 64 μL of diluted liposomal preparation (lipid/DNA ratios of 1/1, 2/1, 3/1, 4/1, 5/1, and 8/1). The vials were tapped gently for 1 min to ensure proper mixing, and then allowed to rest at room temperature for 30 min for proper lipoplex compaction. The volume of all lipoplex suspensions was adjusted with nuclease-free water to 150 μL. This lipoplex stock solution was used for both gel electrophoresis and size/zeta potential measurements.

Gel electrophoresis of lipoplexes: In the gel electrophoresis experiment an amount of 15 μL of each lipoplex formulation was aliquoted out in small eppendorf vials and each vial subsequently received 3 μL of Blue/Orange Loading dye (Promega). A DNA standard was made by mixing 2 μL of diluted DNA stock with 13 μL nuclease free water and 3 μL of Blue/Orange Loading dye. The same procedure was used to make a ladder reference standard using the Lambda DNA/*Hin*d III marker. The final volume in all vials was 18 μL. The lipoplex/dye mixtures were loaded into a 1% Agarose gel in 1X TAE buffer, pre-stained with GelStar® (Lonza) nucleic acid stain (10 μL in 50 mL gel suspension). Gel electrophoresis was carried out at 75 mV for 75 min. DNA bands were visualized with a Mighty Bright transilluminator (Hoefer), and the gel was photographed with an Olympus C-5060 digital camera.

Lipoplex characterization: The remaining 135 μL from each lipoplex preparation was diluted to a final volume of 600 μL with nuclease-free water and transferred into a

disposable Malvern DTS 1060 measurement cell. The size and zeta potential of the lipoplexes were measured using a Zetasizer Nano (Malvern Instruments) at 25°C at normal resolution. Volume results were used for size data, and results were reported as the average of 10–20 runs. Zeta potentials were measured in millivolts (mV) and the average was taken of 10–20 runs.

General procedure for transfection and cytotoxicity experiments

Preparation of lipoplexes: In a typical experiment, for each cationic liposomal formulation to be tested an amount of 3 μL of a 0.5 mg/mL gWiz™ Luc plasmid DNA solution was aliquoted out in a sterile eppendorf tubes and was diluted with 13 μL nuclease-free water. The diluted DNA was then treated with 144 μL of the liposomal formulation (0.1 mM total cationic charge), prepared as indicated above. The vials were tapped gently to ensure proper mixing, and then allowed to rest at room temperature for 30 min for complete lipoplex compaction. This lipoplex stock solution was used for transfection, cytotoxicity, size, and zeta potential measurements.

Transfection and viability experiments: From the lipoplex stock solution, an amount of 135 μL was aliquoted out for each cationic lipid formulation to be tested, and was diluted with 765 μL Optimem (GibcoBRL).

The lipoplexes were tested for their ability to transfect NCI-H23 cancer cell lines. The cells were maintained in 10% fetal bovine serum (FBS) enriched medium at 37 °C in a humidified atmosphere of 95% air/5% CO_2. The media RPMI 1640 (CellGro, Houston, TX) was used for NCI-H23. Twenty-four hours prior to transfection, cells were transferred to 96-well microtiter plates (Cellstar 655180, Greiner Bio-One) at a density of 20,000 cells/well. Each well received 100 μL of appropriate medium, and the plate was incubated in the same conditions as above. All experiments were done in quadruplicate. Two plates were made for each experiment: one for transfection and one for cytotoxicity. The error bars in figures represent one standard deviation from the average value.

Immediately before transfection the medium was removed and the cells from each well were briefly washed with 200 μL sterile PBS. After removal of the PBS solution each well received 100 μL of lipoplex stock solution, and the plates were returned to the incubator. After 90 min incubation time with cells the lipoplex suspension was removed, cells were washed with sterile PBS and then each well received 200 μL of medium. Cell plates were incubated for further 48 hours, after which the transfection efficacy was determined using the first cell plate and the associated cytotoxicity was assessed using the second cell plate, transfected in similar conditions as the first one.

Transfection efficiency: luciferase and protein content assay: Forty-eight hours after transfection, the medium was aspirated and the wells were washed briefly with 200 μL PBS. After removal of PBS the cells were lysed by adding 100 μL 1X reporter lysis buffer (Promega) to each well and incubating the plate at 37 °C for 15 minutes. The cell lysate was collected and used for luciferase and protein assays.

For the luciferase assay, 20 μL of cell lysate was transferred to a test tube and assessed directly by means of BD Monolight 3010 luminometer (BD Biosciences, San Jose, CA) using a luciferase assay kit (E4030) from Promega.

The protein content was quantified using a bicinchoninic acid (BCA) assay (Thermo Scientific, Rockford, IL). The BCA assay was prepared as specified in its manufacturer's instructions; 40 μL of cell lysate were treated with 1 mL of BCA reagent in an acryl cuvette and the solution was incubated for 1 hour at 37 °C. The light absorption of the solution was then read at 562 nm by means of a Hach DR/4000U UV-VIS Spectrometer (Loveland, CO), and the protein content was estimated by comparison to bovine serum albumin standards. The luciferase activity was normalized by the protein content and expressed as relative luminescence units/Ng of protein (RLU/Ng protein).

Viability assay: In order to quantify the relative cytotoxicity of the non-viral cationic vectors, a WST-1 standard viability method[37] was performed along with the luciferase and BCA assays. Forty-eight hours post-transfection, 20 μL of WST-1 tetrazolium dye solution (Roche, Mannheim, Germany) was added to each well (still containing 200 μL of medium). A blank was prepared by mixing 200 μL of medium and 20 μL of tetrazolium dye solution, and the plate was incubated at 37 °C in the CO_2 incubator. After 3 hours the colorimetric measurement was performed at 450 nm (with a reference wavelength of 650 nm that was subtracted) by means of a SpectramaxM2 microplate reader (Molecular Devices, Sunnyvale, CA). The value corresponding to the blank was deducted from the value corresponding to each well. Viability was expressed as percentage of the control, represented by cells that underwent the same treatments but did not receive any cationic lipoplexes.

Lipoplex characterization: The remaining 25 μL from each lipoplex preparation was diluted to a final volume of 500 μL with nuclease-free water and transferred into a disposable Malvern DTS 1060 measurement cell. The size and zeta potential of the lipoplexes were measured using a Zetasizer Nano (Malvern Instruments) at 25°C at normal resolution. Volume results were used for size data, and results were reported as the average of 10–20 runs. Zeta potentials were measured in millivolts (mV).

3D Transfection—NCI-H23 lung cancer, HT29 and HCT116 colon cancer cell lines were grown in RPMI-1640 media supplemented with 10% FBS in A-U96 Lipidure® plates (NOF, Tokyo, Japan) starting with a density of 1000 cells/200 μL. Spheroid formation was observed in about two-three days, and their growth was followed and imaged. After eighteen days each spheroid (about 0.7 mm in diameter and containing about 40000 cells) was transfected by directly adding 14 μL lipoplex suspension prepared in the same way as described above in the well. The transfection media contained the same amount of DNA as in the monolayer transfection experiment presented above (0.14 μg/well). Two plasmids, gWizLuc and gWizGFP were used in parallel experiments. After 3 days each spheroid was transferred into an eppendorf tube, washed with PBS and imaged for GFP expression via confocal fluorescence microscopy or lysed with reporter lysis buffer 1X overnight and assessed for luciferase content, as described above. In the case of GFP measurements the washed spheroids were placed on a coverslip and GFP expression was visualized by laser scanning confocal microscopy using a Carl Zeiss 710 two-photon confocal microscope

equipped with a W Plan-Apochromat 10X air objective, using 0.9X digital zoom, with excitation at 488 nm. 3D transfection images were generated by z-stacking individual 2D images using Zen 2010 Software as previously described.[38,39]

Lipoplex internalization experiments - investigation of mechanisms/routes of internalization—Twenty-four hours prior to transfection, NCI-H23 cells were transferred to 96-well microtiter plates (Cellstar 655180, Greiner Bio-One) at a density of 20,000 cells/well. Each well received 100 μL of RPMI-1640 containing 10% FBS, and the plate was incubated overnight in the same conditions as above. All experiments were done in quadruplicate. The next day the media was removed and cells were washed with warm PBS. After PBS removal each well received 100 μL stock solution of either chloropromazine hydrochloride (10 μg/mL),[40,41] genistein (200 μM)[40,42–44] or EIPA 100 μM[45,46] in serum free culture media for 1 hour at 37 °C. Subsequently, 100 μL lipoplexes were added and typical transfection procedure was conducted as described above. The transfection values obtained in the presence of cell internalization inhibitors were divided by the transfection values obtained in the absence of inhibitors (control experiment) and reported as percentage of these control values.

In a parallel experiment, NCI-H23 cells were cultured as presented above, then trypsinized and the cell suspension was centrifuged at 1000 rpm for 3 min; the supernatant was discarded and cells were re-suspended in Optimem at a concentration of 5×10^6 viable cells/mL. A volume of 0.8 mL cell suspension was mixed with 50 μg plasmid DNA encoding the GFP-tagged Rab7 protein (Addgene, Cambridge MA) and was transferred into a 4-mm gap electroporation cuvette. Cells were subsequently electroporated using a Gene Pulser II electroporator (BioRad) at 350 V, 960 microfarads and infinite resistance. The transfected cells were allowed to recover for 3h in Optimem, after which cell suspension was diluted with RPMI-1640 media containing 10% FBS, cells were counted and transferred onto 12 mm glass coverslips in a 24 well plate at a density of about 10^5 cells/well. After 48 h incubation time (37 °C, 5% CO_2) a confluence degree of about 40–60% was obtained (~ 2×10^5 cells/well). Media was removed and cells were washed with PBS and subsequently incubated with 0.5 mL lipoplexes in Optimem generated as described above (see transfection and cytotoxicity experiments). After 90 min incubation time with cells the lipoplex suspension was removed, cells were washed, fixed with 4% formaldehyde in PBS, washed again with PBS and imaged for Rab7-GFP using a Carl Zeiss 510 Meta confocal microscope (Zeiss) with a 40X oil objective using an excitation wavelength of 488 nm. Images were analyzed using Zen 2010 (Zeiss).

Statistical analysis—Statistical comparisons were performed by analysis of variance (ANOVA) using GraphPad Prism 6, where $*P < 0.05$, $**P < 0.01$, $***P < 0.001$ and $****P < 0.0001$ unless specified otherwise.

Results and Discussion

The pyridinium cationic lipid SPYRIT-7, subsequently referred to as “cationic lipid” or “lipid”, and the gemini surfactant SPYRIT-68, subsequently referred to as “gemini surfactant, GS” were synthesized and purified as previously reported.[33,36]

The cationic lipid or its blends with colipids DOPE or cholesterol at 1:1 and 1:2 lipid/colipid molar ratio were hydrated with deionized water through repeated freeze/thaw cycles and subjected to nanoDSC analysis in order to determine the gel/liquid crystalline transition temperature of the pure lipid and the impact of colipid nature and amount on this transition. Similar blends in which 5% of the cationic charge brought by SPYRIT-7 was replaced with the equivalent amount of GS SPYRIT-68 were prepared in parallel and subjected to nanoDSC analysis in order to assess the effect of GS blending on bilayer fluidity. Results are presented in Figure 1.

As one may observe in Figure 1, lipid SPYRIT-7 in hydrated form has a transition temperature around 30 °C. The transition temperature of GS SPYRIT-68 was below 0 °C (data not shown). Addition of either DOPE or cholesterol colipids to SPYRIT-7 bilayers lowers substantially the transition temperature of the resulted lipid mixture with simultaneous broadening of the thermal transition peak, as expected.[47–49] The effect is proportional with the amount of colipid used. On the other hand, replacing 5% of the positive charge brought by the cationic lipid in the cationic bilayer with the same amount of charge of the corresponding amount of GS completely wipes out the remaining (broad) thermal transition of the SPYRIT-7/colipid supramolecular assemblies. Thus, blending of GS has an additional leveling effect on the gel/liquid crystalline thermal transition of the lipid mixture, acting synergistically with the colipid towards fluidizing (laterally) the cationic bilayer. All ternary amphiphile mixtures are perfectly fluid over a wide range of temperatures (Figure 1).

The above-mentioned hydrated cationic blends were subsequently sonicated to generate cationic liposomes. Since the gemini surfactant has a lower packing parameter (higher molecular curvature) than cationic lipid, it was expected that ternary lipid mixtures containing GS would be able to adapt higher bilayer curvatures and to yield smaller liposomes as compared with binary mixtures of SPYRIT-7 and colipids with equivalent positive charge. In order to test the effect of GS on the size/curvature of cationic liposomes, the ternary mixtures containing either 5% or 10% GS (but the same overall amount of positive charge) were made, in addition to the binary cationic lipid/colipid mixtures indicated above. The size and zeta potential of the resulted vesicles are presented in Figure 2 (panels a, c). An analysis of the data of Figure 2 reveals that the size of SPYRIT-7/Chol (1/1 and 1/2 molar ratio) liposomes was generally bigger than the size of SPYRIT-7/DOPE corresponding liposomes. Importantly, the effect of GS blending into cationic lipid/colipid formulations also depends on the nature of co-lipid used: for DOPE-based liposomes addition of 5% GS does not change significantly the size of the vesicles (d ~ 250 nm), while a significant decrease in size is observed for cholesterol-based liposomes (from 600 nm to about 250–300 nm). It appears that the more flexible DOPE can accommodate the small increase of the positive curvature of the bilayer induced by GS while the more rigid cholesterol cannot do that. Interestingly, doubling the amount of GS blended into bilayers *increases* the sizes of the liposomes from ~ 250 nm to 600–900 nm, with the exception of cationic amphiphiles/cholesterol 1:2 formulation, where the size of the vesicles decreases to 250 nm, as initially expected. We hypothesize that the increase in size of the supramolecular assemblies at 10 % GS after an initial decrease at 5% GS is due either to different

amphiphile distribution in the two bilayer leaflets at the two GS concentrations or to a liposome to worm micelle transition when passing from 5% to 10% GS in the cationic blend. The results of a parallel experiment of blending DOPE into a 10GS/90lipid cationic mix (Figure 2, panel b) support the first hypothesis since the size of supra-molecular aggregates increases monotonously from 400 nm to 900 nm with the increase of colipid molar fraction in the mix up to 50%, after which it decreases to about 600 nm when the amount of colipid is doubled. The possible bilayer asymmetry can explain also the variable results observed for the zeta potential of the 10GS/90lipid assemblies with variable DOPE content (Figure 2d), which increased from + 45 mV to about + 60 mV. For the other lipid blends the zeta potential decreased from ~ + 60–65 mV to + 50 mV when the amount of GS in the blend was reduced. This trend is normal since the charge density of GS SPYRIT-68 is higher than the corresponding charge density of cationic lipid SPYRIT-7 (the charge per mass ratio is in favor of GS) (Figure 2c, 2d).

The cationic formulations presented above were tested for their ability to compact plasmid DNA encoding the luciferase gene (gWizLuc, Aldevron). The compaction process was followed at different cationic amphiphile/DNA +/− charge ratios (Figure 3) by monitoring the size (Figure 3a), zeta potential (Figure 3b) and electrophoretic mobility (Figure 3c) of lipoplexes generated from each cationic amphiphile-based co-formulation used.

When the cationic lipid was formulated alone, no full compaction of the DNA could be observed (data not shown). This is probably due to the very high positive charge density in the cationic bilayer that causes strong repulsions between the cationic heads, destabilizing the bilayer and preventing the formation of stable DNA complexes.[47]

However, efficient compaction of DNA was observed when SPYRIT-7 cationic lipid was formulated with either DOPE or cholesterol, as seen in Figure 3 (red bars, and top row of gels). The compaction process was dependent on the nature of co-lipid used (DOPE or cholesterol), on its molar ratio to cationic lipid (1:1 or 1:2), and on the cationic lipid/DNA charge ratio. For lipoplexes obtained from SPYRIT-7/ DOPE (1:1) formulation, *full compaction of DNA* occurred at cationic lipid/ DNA charge ratio between 3 and 4, as revealed by the positive shift in zeta potential and the gel electrophoresis mobility experiment. At these charge ratios a significant drop in the size of the lipoplexes from 800 nm to ~ 350 nm could also be observed in the majority of cases. At higher charge ratios, the zeta potential continued to increase to + 25 mV while the size continues to decrease, reaching a minimum average size for the complexes of 219 nm. Interestingly, the supercoiled plasmid (lower DNA band) is compacted faster than the relaxed circular DNA (Figure 3c, upper left panel). A possible explanation is that the supercoiled DNA is compacted with a larger amount of counterions (thus requiring less cationic amphiphile) than the relaxed plasmid, similarly with the mechanism proposed recently by Aicart and Bhattacharya for the compaction of (supercoiled) plasmid DNA versus linear DNA.[50] When the molar ratio of DOPE was increased (cationic lipid/DOPE 1:2 formulation), the additional co-lipid caused full DNA compaction to occur at a cationic lipid/DNA charge ratio between 2 and 3 but the decrease in lipoplex size after compaction was less abrupt than for lipoplexes based on cationic lipid/DOPE 1:1 lipid mixtures. The zeta potential was 21.3 mV at the same charge ratio (3), significantly higher than the zeta potential for the above-mentioned

lipoplexes. These results are in good agreement with the results obtained recently by Aicart and Bhattacharya for DNA compaction with cationic gemini surfactants/DOPE formulations.[51]

While analyzing the lipoplexes derived from SPYRIT-7/cholesterol formulation (1:1 molar ratio) one may observe that *full DNA compaction* did not occur even at high charge ratios. The zeta potential turned positive around a charge ratio of 5, when the size of lipoplexes decreases abruptly from 1218 nm to 412 nm. Doubling the amount of cholesterol in the liposomal formulation leads to (lateral) fluidization of the cationic bilayer (as presented in Figure 1) and decreases the +/− charge ratio at which DNA is compacted to 4, with a size of corresponding lipoplexes of 346 nm.

Substituting 5% of the positive charge brought by cationic lipid SPYRIT-7 in above mentioned formulations with the same amount of positive charge from gemini surfactant SPYRIT-68 had a significant effect on the corresponding lipoplex properties (Figure 3, green bars and second row of gels). Thus, DNA compaction occurred at lower charge ratios (2 for cationic lipid/DOPE 1/1 and 1/2, 3 for cationic lipid/cholesterol 1/1 and 2 for cationic lipid/cholesterol 1/2) as indicated by zeta potential shifts to positive values and confirmed by lipoplex electrophoretic mobility. The size of lipoplexes at full DNA compaction decreased for all formulations, revealing a more compact structure. In the case of lipoplexes generated from SPYRIT-7/DOPE 1/2 and SPYRIT-7/cholesterol 1/2 the supercoiled DNA was compacted faster than the relaxed one. We hypothesize that lateral movement of gemini surfactant in the fluid bilayers allows its concentration in areas where the DNA makes high curvature loops otherwise difficult to accommodate by the less flexible cationic lipid congener. This mechanism is probably responsible for the monotonous decrease in size of lipoplexes while increasing the charge ratio observed for GS-containing lipoplexes, as opposed to dramatic size contractions observed in the case of lipoplexes derived from formulations containing exclusively cationic lipid SPYRIT-7.

Increasing the percentage of positive charge brought by gemini surfactant into the cationic amphiphile blend to 10% has a further beneficial effect: the minimum charge ratio required for DNA compaction continues to decrease, the lipoplex zeta potential is most of the times higher as compared with GS/lipid 5/95 blends and the DNA is better compacted (Figure 3 violet bars and third row of gels). DNA in DOPE-containing lipoplexes 10GS_90lipid/DOPE 1/1 is fully compacted at a +/− charge ratio of 1 for lipoplexes derived from 10GS_90lipid/DOPE 1/1) a feature that is a rather rare in cationic lipid-mediated transfection. For lipoplexes derived from 10GS_90lipid/DOPE 1/2 the supercoiled DNA is fully compacted at +/− charge ratio of 1, while a small amount of free circular plasmid still can be observed at this charge ratio. The same observations are also valid for cholesterol-containing lipoplexes, where the percent of uncompacted DNA is dramatically reduced when 10% GS is blended into the cationic amphiphile mixture.

In order to test the effect of GS blending towards the transfection efficiency of the lipoplexes, we assessed the above-mentioned DNA complexes prepared at the +/− charge ratio of 3 against the NCI-H23 cell line. This cell line proved very susceptible to be transfected by pyridinium amphiphiles[13,33] thus allowing the fine quantization of the

differences in transfection efficiency of different formulations. The cytotoxic effect associated with transfection process was quantified in parallel using a WST-1 viability assay (Figure 4). Lipoplexes generated from commercial transfection agent Lipofectamine® at the same charge ratio of 3 were added as reference. The size and zeta potentials of the lipoplexes were in good agreement with the ones found in the optimization study (Figure 3) with DOPE-containing lipoplexes having slightly smaller sizes as compared to cholesterol containing ones (Figure 4a). The zeta potential of all formulations was positive at this charge ratio within experimental errors (Figure 4c) and in good agreement with the values obtained in the optimization study (Figure 3). The standard transfection agent Lipofectamine generated lipoplexes with a size of 250 nm and a zeta potential of 2 mV.

In terms of transfection efficiency it can be observed that cholesterol-based lipoplexes were more efficient than DOPE-based ones at similar cationic species composition. The molar ratio of colipid in the formulation proved also important. Increasing the DOPE content of the DOPE-based lipoplexes had a beneficial effect on transfection efficiency while an increase of cholesterol molar ratio in the cholesterol-based lipoplexes decreased the transfection efficiency of corresponding DNA complexes. Lipoplexes derived from SPYRIT-7/chol 1/1 formulation were found to be equal or more efficient than Lipofectamine, confirming the conclusions of previous studies.[33] Importantly, lipoplexes derived from cationic blends containing 5 % positive charge brought by gemini surfactant SPYRIT-68 were 2–3 times more efficient than the corresponding lipoplexes generated from 100% cationic lipid, revealing a significant impact of the gemini surfactant on transfection efficiency. Lipoplexes derived from 5GS_95lipid/chol 1/1 and 1/2 were several times more efficient than Lipofectamine, while lipoplexes derived from 5GS_95lipid/DOPE 1/1 and 1/2 matched the efficiency of this standard transfection system. Interestingly, doubling the charge contribution of the gemini surfactant in the lipoplexes did not increase further the transfection efficiency; in fact the efficiency of the lipoplexes containing 10% positive charge from GS was inferior to the efficiency of lipoplexes derived only from SPYRIT-68 (Figure 4e), with the 10/90 GS/lipid: DOPE formulations being practically devoid of transfection efficiency. We hypothesize that the GS is favoring the fusion of the lipoplex with the endosomal membrane due to its high curvature and elastic modulus and high charge density, as presented by Safinya's group.[22] Similar fusogenic properties are induced into lipoplexes by DOPE through its ability to adopt an inverted hexagonal phase. However, the packing parameters of GS SPYRIT-68 and DOPE are quite opposite and we suspected that the two amphiphiles may cancel each other in terms of fusogenicity. Therefore we tested the effect of reducing the DOPE amount in the 10/90 GS/lipid blends (Figure 4b, 4d, 4f, 4h). Data from Figure 4f reveals that the transfection efficiency of 10/90 GS/lipid blends can be regained by reducing the DOPE amount. Interestingly, the 10/90 cationic GS/lipid blends were efficient in the absence of any colipid, being able to condense DNA into 400 nm lipoplexes with positive zeta potential (Figure 4b, 4d, 4f). One may also observe the excellent cytotoxic profile of the lipoplexes, irrespective of their composition. The experiment reveals the ability of gemini surfactant SPYRIT-68 to potentiate transfection without raising the cytotoxicity of the formulation, thus validating the working hypothesis.

We also assessed the ability of the most efficient formulations towards transfecting tumor spheroids in vitro. Spheroids derived from lung carcinoma cell line NCI-H23 and from two

colon carcinomas – HT-29 and HCT-116 were grown to ~ 0.7 mm diameter, when they are thought to contain about 40000 cells (the same amount of cells transfected in a well in the 96-well plate format). We incubated the individual spheroids with lipoplexes generated under the same conditions as in the 2D experiment and containing the same amount of DNA/cell. Besides luciferase we also used the gWizGFP plasmid, which allows a better visualization of the transfected cells in 3D after confocal imaging and reconstruction of the three-dimensional image from sequential 2D ones (Figure 5). Data from Figure 5 revealed an interesting trend, with the DOPE-based formulation superior to the cholesterol-based ones irrespective of the reporter gene plasmid used. Luciferase data (Figure b) mirrored the results obtained with GFP plasmid. The transfection was cell-type dependent, with the NCI-H23 spheroids being the most susceptible to be transfected and showing the most significant transfection differences, followed by HCT-116 and HT-29. Select GS-based lipoplexes equaled or surpassed Lipofectamine in this experiment too, as revealed by both GFP and luciferase data.

The major transfection differences observed between lipoplexes containing variable amounts of GS SPYRIT-68 and between the 2D and 3D transfection experiments prompted us to assess the implication of GS in another delivery barrier, namely the cellular internalization of the lipoplexes. Several mechanism of lipoplex internalization are known, including clathrin- and caveolae-mediated endocytosis and (macro)pinocytosis, which can be selectively blocked by chloropromazine, genistein, and 5-(N-ethyl-N-isopropyl)amiloride (EIPA).[52–56] We tested the internalization mechanism used by the most efficient pyridinium lipoplexes using the same NCI-H23 lung cancer cell line and the three above-mentioned selective inhibitors. Specifically, transfection efficiency of lipoplexes generated from cationic amphiphile(s)/DOPE (1/2 molar ratio) and cationic amphiphile(s)/cholesterol (1/1 and 1/2 molar ratios) formulations, containing 0%, 5% and 10% positive charge contributed by GS SPYRIT-68, prepared at a charge ratio of 3 as previously done, was assessed in the absence and in the presence of (i) chloropromazine (10 μg/mL), (ii) genistein (200 μM), and (iii) EIPA(100 μM) (Figure 6). Data from Figure 6 revealed that the cellular uptake, measured as the ratio between the transfection efficiency in the presence of internalization inhibitors over the transfection efficiency in normal conditions (control experiment), was strongly dependent on the composition of the lipoplexes. Thus, the DOPE-containing lipoplexes are internalized primarily through pinocytosis (inhibited by EIPA). Addition of GS SPYRIT-68 does not change the primary mechanism of internalization, but it may open an alternative caveolae-mediated endocytosis pathway (inhibited by genistein) which is dependent on the amount of GS in the formulation (Figure 6A). This availability of this pathway is controlled by the amount of fusogenic component (either GS or DOPE) in the lipoplex. On the other hand, cholesterol-containing lipoplexes derived from SPYRIT-7 use all three internalization pathways. For lipoplexes rich in cholesterol (cationic amphiphile/cholesterol molar ratio of 1:2) the blending of GS SPYRIT-68 does not have a significant effect on the internalization pathways.

However, a very different trend emerges for lipoplexes derived from cationic amphiphile/cholesterol formulated at 1:1 molar ratio: blending of GS SPYRIT-68 causes the simultaneous suppression of cellular uptake throughout all three pathways, in a dose-dependent manner (Figure 6a). Taking into account that these formulations were the most

efficient in 2D transfection experiments, we can conclude that addition of the GS SPYRIT-68 into the lipoplexes triggers their internalization through another mechanism. A possible mechanism is through temporary poration of external membranes by the GS [22]. This fact might explain the different transfection trends observed between two-dimensional and three-dimensional transfection experiments. Consequently, the internal membranes of endolysosomes should be affected in the same way by the GS-containing lipoplexes still internalized through classical pathways investigated above. In order to test this hypothesis we transfected NCI-H23 cells with Rab-7 protein labeled with GFP using the electroporation technique. This protein (a small GTPase) is specific for endolysosomes and does not exist in caveolae and in the vesicles internalized from plasmalemma [57, 58]. Forty eight hours post-transfection with Rab-7 the cells were incubated 2h with lipoplexes that did not contain GS and that contained 5% charge brought by GS, after which they were washed, fixed with 4% paraformaldehyde, washed and imaged immediately via confocal microscopy for Rab-7 intracellular distribution against control cells that did not receive lipoplexes (Figure 7). Analyzing the data from Figure 7 one can observe that NCI-H23 cells that did not receive lipoplexes display a Rab-7 intracellular distribution limited to endolysosomes (left panels) and that the transfection with lipoplexes that do not contain GS SPYRIT-68 does not alter significantly the Rab-7 intracellular distribution. However, the lipoplexes containing 5 % GS promote endolysosomal membrane rupture and release of Rab-7 (and of DNA cargo) into the cytoplasm (Figure 7, right panels). The diffuse cytoplasm distribution of Rab-7 supports the proposed temporary poration of external and internal membrane by GS-containing formulations.

This study demonstrated that the addition of pyridinium gemini surfactant SPYRIT-68 to cationic bilayers formed by pyridinium cationic lipid SPYRIT-7 acts synergistically with co-lipids DOPE or cholesterol towards fluidizing completely the supramolecular amphiphile assembly. Blending of gemini surfactant into the cationic lipid-based bilayers can impact substantially the size and, to some extent, the zeta potential of the vesicles formed from these hydrated bilayers upon sonication. The mixed cationic amphiphile assemblies were able to fully compact plasmid DNA at lower +/− charge ratios, generate lipoplexes of smaller size and higher zeta potential as compared with corresponding cationic bilayers of equivalent positive charge containing only cationic lipid SPYRIT-7. These observations, in concert with the fluctuation observed for the size of resulting lipoplexes while increasing the cationic amphiphile/DNA charge ratio in the absence and in the presence of gemini surfactant, strongly indicate a different compaction mechanism in which the gemini surfactant concentrates in areas where DNA makes high curvature loops otherwise difficult to accommodate by the less flexible cationic lipid congener at the same +/− charge ratio. Moreover, the addition of pyridinium GS can enhance dramatically the transfection efficiency of SPYRIT-7 cationic lipid-based formulations, surpassing standard commercial transfection systems while displaying negligible cytotoxicity, as revealed by 2D- and 3-D transfection experiments. Blending of gemini surfactant SPYRIT-68 into cationic lipid SPYRIT-7-based lipoplexes can also change substantially the internalization mechanism of the lipoplexes. The overall impact depends heavily on the presence of co-lipids, their nature and amount present into the lipoplexes, with most susceptible formulations being the ones containing cholesterol in equimolar amount to cationic lipids. The study confirmed the

possibility of combining the specific properties of pyridinium gemini surfactants and cationic lipids synergistically for obtaining synthetic transfection systems with improved transfection efficiency and negligible cytotoxicity useful for therapeutic gene delivery.

Acknowledgments

Financial support from the NSF (CHE-0923077), NIH (HL 09804), Temple University – Provost's Office, Temple Undergraduate Research Program, Temple University School of Pharmacy- Dean's Office is gratefully acknowledged. V. D. S. acknowledges the receipt of a graduate scholarship from Temple University Graduate School.

Abbreviation list

ANOVA	analysis of variance
BCA	Bicinchoninic acid
Chol	Cholesterol
DOPE	Dioleoylphosphatidylethanolamine
DLS	Dynamic light scattering
EIPA	5-(*N*-ethyl-*N*-isopropyl) amiloride
DNA	Deoxyribonucleic acid
DSC	Differential scanning calorimetry
FBS	Fetal bovine serum
GFP	Green fluorescent protein
GS	Gemini surfactant
PBS	Phosphate buffer saline
RNA	Ribonucleic acid
siRNA	small interfering RNA
WSTs	Water soluble tetrazolium salts

References

1. Dotti, G.; Savoldo, B.; Okur, F.; Rousseau, RF.; Brenner, MK. Gene Cell Ther. 3. 2009. Gene therapy for the treatment of cancer: from laboratory to bedside; p. 1001-1018.
2. Kay MA. State-of-the-art gene-based therapies: the road ahead. Nat Rev Genet. 2011; 12:316–328. [PubMed: 21468099]
3. Mingozzi F, High KA. Therapeutic in vivo gene transfer for genetic disease using AAV: progress and challenges. Nat Rev Genet. 2011; 12:341–355. [PubMed: 21499295]
4. Li SD, Huang L. Non-viral is superior to viral gene delivery. J Control Release. 2007; 123:181–183. [PubMed: 17935817]
5. Li W, Szoka FC Jr. Lipid-based nanoparticles for nucleic acid delivery. Pharm Res. 2007; 24:438–449. [PubMed: 17252188]
6. Ewert K, Ahmad A, Evans HM, Safinya CR. Cationic lipid-DNA complexes for non-viral gene therapy: relating supramolecular structures to cellular pathways. Expert Opin Biol Ther. 2005; 5:33–53. [PubMed: 15709908]

7. Ilies, MA.; Sommers, TV.; He, LC.; Kizewski, A.; Sharma, VD. Amphiphiles: Molecular Assembly and Applications. Nagarajan, R., editor. ACS Symposium Series; Washington, DC: 2011. p. 23-38.
8. Pinnaduwage P, Schmitt L, Huang L. Use of a quaternary ammonium detergent in liposome mediated DNA transfection of mouse L-cells. Biochim Biophys Acta. 1989; 985:33–37. [PubMed: 2790044]
9. Sharma VD, Ilies MA. Heterocyclic Cationic Gemini Surfactants: A Comparative Overview of Their Synthesis, Self-Assembling, Physicochemical, and Biological Properties. Medicinal Research Reviews. 2014; 34:1–44. [PubMed: 22907528]
10. Menger FM, Keiper JS. Gemini surfactants. Angew Chem Int Ed Engl. 2000; 39:1907–1920.
11. Kirby AJ, Camilleri P, Engberts JBFN, Feiters MC, Nolte RJM, Soderman O, Bergsma M, Bell PC, Fielden ML, Rodriguez CLG, Guedat P, Kremer A, McGregor C, Perrin C, Ronsin G, van Eijk MCP. Gemini surfactants: New synthetic vectors for gene transfection. Angew Chem Int Ed Engl. 2003; 42:1448–1457. [PubMed: 12698476]
12. Wettig SD, Verrall RE, Foldvari M. Gemini surfactants: A new family of building blocks for non-viral gene delivery systems. Curr Gene Ther. 2008; 8:9–23. [PubMed: 18336246]
13. Ilies MA, Seitz WA, Johnson BH, Ezell EL, Miller AL, Thompson EB, Balaban AT. Lipophilic pyrylium salts in the synthesis of efficient pyridinium-based cationic lipids, gemini surfactants, and lipophilic oligomers for gene delivery. J Med Chem. 2006; 49:3872–3887. [PubMed: 16789743]
14. Bhattacharya S, Bajaj A. Advances in gene delivery through molecular design of cationic lipids. Chem Commun. 2009:4632–4656.
15. Zhang XX, McIntosh TJ, Grinstaff MW. Functional lipids and lipoplexes for improved gene delivery. Biochimie. 2012; 94:42–58. [PubMed: 21621581]
16. Mintzer MA, Simanek EE. Nonviral vectors for gene delivery. Chem Rev. 2009; 109:259–302. [PubMed: 19053809]
17. Radler JO, Koltover I, Salditt T, Safinya CR. Structure of DNA-cationic liposome complexes: DNA intercalation in multilamellar membranes in distinct interhelical packing regimes. Science. 1997; 275:810–814. [PubMed: 9012343]
18. Koltover I, Salditt T, Radler JO, Safinya CR. An inverted hexagonal phase of cationic liposome-DNA complexes related to DNA release and delivery. Science. 1998; 281:78–81. [PubMed: 9651248]
19. Israelachvili JN, Mitchell DJ, Ninham BW. Theory of Self-Assembly of Hydrocarbon Amphiphiles into Micelles and Bilayers. J Chem Soc Farad Trans 2. 1976; 72:1525–1568.
20. Nagarajan R. Molecular packing parameter and surfactant self-assembly: The neglected role of the surfactant tail. Langmuir. 2002; 18:31–38.
21. Nagarajan R, Ruckenstein E. Theory of Surfactant Self-Assembly - a Predictive Molecular Thermodynamic Approach. Langmuir. 1991; 7:2934–2969.
22. Lin AJ, Slack NL, Ahmad A, George CX, Samuel CE, Safinya CR. Three-dimensional imaging of lipid gene-carriers: Membrane charge density controls universal transfection behavior in lamellar cationic liposome-DNA complexes. Biophys J. 2003; 84:3307–3316. [PubMed: 12719260]
23. Zhang Y, Anchordoquy TJ. The role of lipid charge density in the serum stability of cationic lipid/DNA complexes. Biochim Biophys Acta. 2004; 1663:143–157. [PubMed: 15157617]
24. Crook K, Stevenson BJ, Dubouchet M, Porteous DJ. Inclusion of cholesterol in DOTAP transfection complexes increases the delivery of DNA to cells in vitro in the presence of serum. Gene Ther. 1998; 5:137–143. [PubMed: 9536275]
25. Ilies MA, Johnson BH, Makori F, Miller A, Seitz WA, Thompson EB, Balaban AT. Pyridinium cationic lipids in gene delivery: an in vitro and in vivo comparison of transfection efficiency versus a tetraalkylammonium congener. Arch Biochem Biophys. 2005; 435:217–226. [PubMed: 15680924]
26. Lindberg MF, Carmoy N, Le Gall T, Fraix A, Berchel M, Lorilleux C, Couthon-Gourves H, Bellaud P, Fautrel A, Jaffres PA, Lehn P, Montier T. The gene transfection properties of a lipophosphoramidate derivative with two phytanyl chains. Biomaterials. 2012; 33:6240–6253. [PubMed: 22672835]

27. Berchel M, Le Gall T, Couthon-Gourves H, Haelters JP, Montier T, Midoux P, Lehn P, Jaffres PA. Lipophosphonate/lipophosphoramidates: a family of synthetic vectors efficient for gene delivery. Biochimie. 2012; 94:33–41. [PubMed: 21840369]
28. Montier T, Benvegnu T, Jaffres PA, Yaouanc JJ, Lehn P. Progress in cationic lipid-mediated gene transfection: a series of bio-inspired lipids as an example. Curr Gene Ther. 2008; 8:296–312. [PubMed: 18855628]
29. Midoux P, Pichon C, Yaouanc JJ, Jaffres PA. Chemical vectors for gene delivery: a current review on polymers, peptides and lipids containing histidine or imidazole as nucleic acids carriers. Br J Pharmacol. 2009; 157:166–178. [PubMed: 19459843]
30. van der Woude I, Wagenaar A, Meekel AA, ter Beest MB, Ruiters MH, Engberts JB, Hoekstra D. Novel pyridinium surfactants for efficient, nontoxic in vitro gene delivery. Proc Natl Acad Sci USA. 1997; 94:1160–1165. [PubMed: 9037023]
31. Meekel AAP, Wagenaar A, Smisterova J, Kroeze JE, Haadsma P, Bosgraaf B, Stuart MCA, Brisson A, Ruiters MHJ, Hoekstra D, Engberts JBFN. Synthesis of pyridinium amphiphiles used for transfection and some characteristics of amphiphile/DNA complex formation. Eur J Org Chem. 2000:665–673.
32. Ilies MA, Seitz WA, Caproiu MT, Wentz M, Garfield RE, Balaban AT. Pyridinium-Based Cationic Lipids as Gene-Transfer Agents. Eur J Org Chem. 2003:2645–2655.
33. Ilies MA, Seitz WA, Ghiviriga I, Johnson BH, Miller A, Thompson EB, Balaban AT. Pyridinium cationic lipids in gene delivery: A structure-activity correlation study. J Med Chem. 2004; 47:3744–3754. [PubMed: 15239653]
34. Scarzello M, Chupin V, Wagenaar A, Stuart MC, Engberts JB, Hulst R. Polymorphism of pyridinium amphiphiles for gene delivery: influence of ionic strength, helper lipid content, and plasmid DNA complexation. Biophys J. 2005; 88:2104–2113. [PubMed: 15613636]
35. Balaban, AT.; Seitz, WA.; Ilies, MA.; Thompson, EB.; Garfield, RE.; Johnson, BH.; Miller, AL.; Wentz, MJ. US Pat. 7456197B2. 2008.
36. Sharma VD, Aifuwa EO, Heiney PA, Ilies MA. Interfacial engineering of pyridinium gemini surfactants for the generation of synthetic transfection systems. Biomaterials. 2013; 34:6906–6921. [PubMed: 23768782]
37. Berridge MV, Tan AS, McCoy KD, Wang R. The biochemical and cellular basis of cell proliferation assays that use tetrazolium salts. Biochemica. 1996:14–19.
38. Mallilankaraman K, Gandhirajan RK, Hawkins BJ, Madesh M. Visualization of vascular Ca2+ signaling triggered by paracrine derived ROS. J Vis Exp. 2011; 58:e3511.
39. Madesh M, Hawkins BJ, Milovanova T, Bhanumathy CD, Joseph SK, Ramachandrarao SP, Sharma K, Kurosaki T, Fisher AB. Selective role for superoxide in InsP3 receptor-mediated mitochondrial dysfunction and endothelial apoptosis. J Cell Biol. 2005; 170:1079–1090. [PubMed: 16186254]
40. Rejman J, Bragonzi A, Conese M. Role of clathrin- and caveolae-mediated endocytosis in gene transfer mediated by lipo- and polyplexes. Mol Ther. 2005; 12:468–474. [PubMed: 15963763]
41. Wang LH, Rothberg KG, Anderson RG. Mis-assembly of clathrin lattices on endosomes reveals a regulatory switch for coated pit formation. J Cell Biol. 1993; 123:1107–1117. [PubMed: 8245121]
42. Liu P, Anderson RG. Spatial organization of EGF receptor transmodulation by PDGF. Biochem Biophys Res Commun. 1999; 261:695–700. [PubMed: 10441488]
43. Aoki T, Nomura R, Fujimoto T. Tyrosine phosphorylation of caveolin-1 in the endothelium. Exp Cell Res. 1999; 253:629–636. [PubMed: 10585286]
44. Rejman J, Oberle V, Zuhorn IS, Hoekstra D. Size-dependent internalization of particles via the pathways of clathrin- and caveolae-mediated endocytosis. Biochem J. 2004; 377:159–169. [PubMed: 14505488]
45. Fretz M, Jin J, Conibere R, Penning NA, Al-Taei S, Storm G, Futaki S, Takeuchi T, Nakase I, Jones AT. Effects of Na+/H+ exchanger inhibitors on subcellular localisation of endocytic organelles and intracellular dynamics of protein transduction domains HIV-TAT peptide and octaarginine. J Control Release. 2006; 116:247–254. [PubMed: 16971016]
46. Nakase I, Niwa M, Takeuchi T, Sonomura K, Kawabata N, Koike Y, Takehashi M, Tanaka S, Ueda K, Simpson JC, Jones AT, Sugiura Y, Futaki S. Cellular uptake of arginine-rich peptides:

roles for macropinocytosis and actin rearrangement. Mol Ther. 2004; 10:1011–1022. [PubMed: 15564133]

47. Farhood H, Serbina N, Huang L. The role of dioleoyl phosphatidylethanolamine in cationic liposome mediated gene transfer. Biochim Biophys Acta. 1995; 1235:289–295. [PubMed: 7756337]
48. Bhattacharya S, Haldar S. The effects of cholesterol inclusion on the vesicular membranes of cationic lipids. Biochim Biophys Acta. 1996; 1283:21–30. [PubMed: 8765090]
49. Bhattacharya S, Haldar S. Interactions between cholesterol and lipids in bilayer membranes. Role of lipid headgroup and hydrocarbon chain-backbone linkage. Biochim Biophys Acta. 2000; 1467:39–53. [PubMed: 10930507]
50. Munoz-Ubeda M, Misra SK, Barran-Berdon AL, Aicart-Ramos C, Sierra MB, Biswas J, Kondaiah P, Junquera E, Bhattacharya S, Aicart E. Why is less cationic lipid required to prepare lipoplexes from plasmid DNA than linear DNA in gene therapy? J Am Chem Soc. 2011; 133:18014–18017. [PubMed: 21985329]
51. Munoz-Ubeda M, Misra SK, Barran-Berdon AL, Datta S, Aicart-Ramos C, Castro-Hartmann P, Kondaiah P, Junquera E, Bhattacharya S, Aicart E. How does the spacer length of cationic gemini lipids influence the lipoplex formation with plasmid DNA? Physicochemical biochemical characterizations and their relevance in gene therapy. Biomacromolecules. 2012; 13:3926–3937. [PubMed: 23130552]
52. Rejman J, Oberle V, Zuhorn IS, Hoekstra D. Size-dependent internalization of particles via the pathways of clathrin- and caveolae-mediated endocytosis. Biochem J. 2004; 377:159–169. [PubMed: 14505488]
53. Rejman J, Bragonzi A, Conese M. Role of clathrin- and caveolae-mediated endocytosis in gene transfer mediated by lipo- and polyplexes. Mol Ther. 2005; 12:468–474. [PubMed: 15963763]
54. Reilly MJ, Larsen JD, Sullivan MO. Polyplexes Traffic through Caveolae to the Golgi and Endoplasmic Reticulum en Route to the Nucleus. Mol Pharmaceut. 2012; 9:1280–1290.
55. Gabrielson NP, Pack DW. Efficient polyethylenimine-mediated gene delivery proceeds via a caveolar pathway in HeLa cells. J Control Release. 2009; 136:54–61. [PubMed: 19217921]
56. Canton I, Battaglia G. Endocytosis at the nanoscale. Chem Soc Rev. 2012; 41:2718–2739. [PubMed: 22389111]
57. Wang T, Ming Z, Xiaochun W, Hong W. Rab7: role of its protein interaction cascades in endo-lysosomal traffic. Cell Signal. 2011; 23:516–521. [PubMed: 20851765]
58. Yu J, Deliu E, Zhang XQ, Hoffman NE, Carter RL, Grisanti LA, Brailoiu GC, Madesh M, Cheung JY, Force T, Abood ME, Koch WJ, Tilley DG, Brailoiu E. Differential activation of cultured neonatal cardiomyocytes by plasmalemmal versus intracellular G protein-coupled receptor 55. J Biol Chem. 2013; 288:22481–92. [PubMed: 23814062]

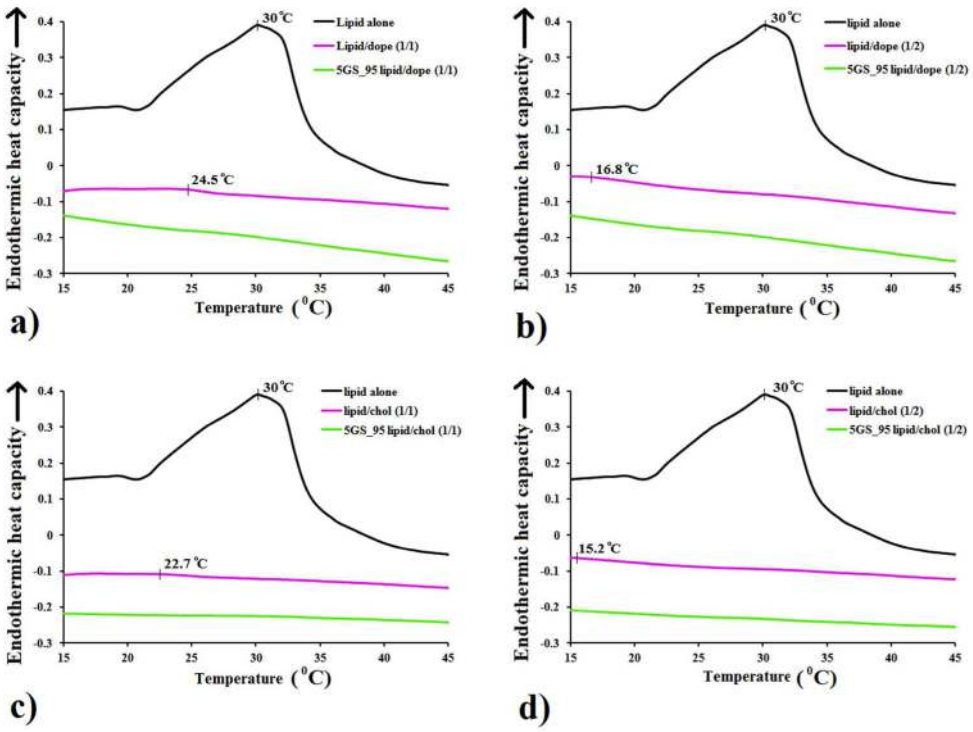

Figure 1.

Comparative nanoDSC traces of cationic lipid SPYRIT-7 (“lipid”) formulated with DOPE (a, b) or cholesterol (c, d) at 1:1 (a, c) and 1:2 (b, d) molar ratios, in water, in the absence (red traces) of in the presence of 5% GS SPYRIT-68 (“GS”, green traces), against the pure cationic lipid formulation (black traces). Broadening and shifting the thermal transition of the cationic lipid to lower values by addition of colipid and subsequent complete bilayer fluidification through GS addition can be observed.

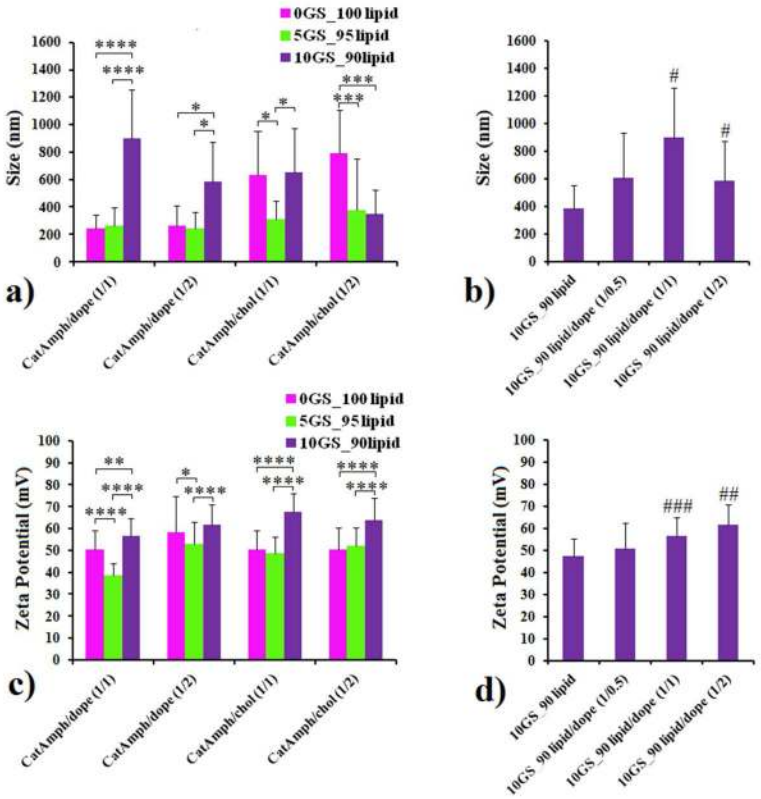

Figure 2.

The impact of GS on the size (panels a, b) and zeta potential (panels c, d) of liposomes generated from SPYRIT-7 cationic lipid and DOPE or cholesterol at 1:1 or 1:2 lipid/colipid molar ratios. Error bars represent s.d. (n = 10–12. P values were determined by two-way ANOVA within one set of formulations (*$P < 0.05$, **$P < 0.01$, ***$P < 0.001$ and ****$P < 0.0001$) or one-way ANOVA, comparing the value with the previous one in the series ($^{\#}P < 0.05$, $^{\#\#}P < 0.01$, $^{\#\#\#}P < 0.001$ and $^{\#\#\#\#}P < 0.0001$). Only the statistical significant differences were shown.

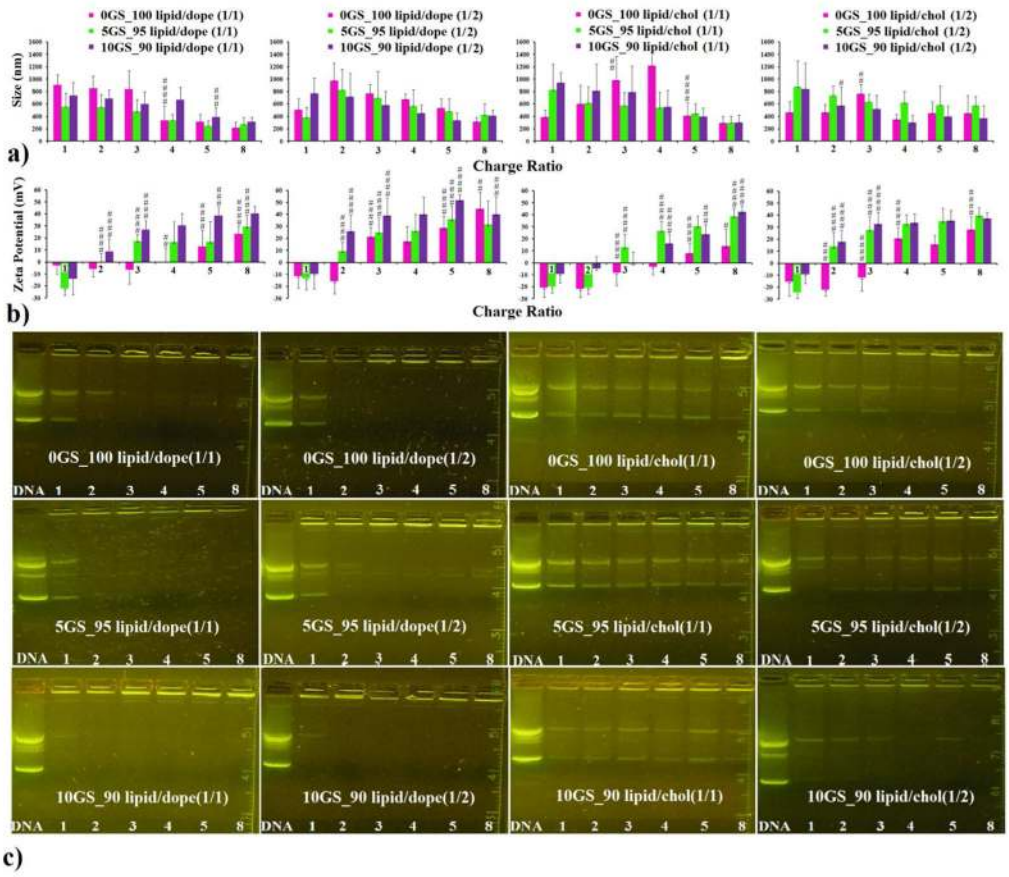

Figure 3.

The compaction of DNA by pyridinium cationic amphiphiles SPYRIT-7 and SYRIT-68, co-formulated with DOPE (1:1 molar ratio, first panel column; 1:2 molar ratio, second panel column) or with cholesterol (1:1 molar ratio, third panel column; 1:2 molar ratio, fourth panel column) depicting the size (a), zeta potential (b) and electrophoretic mobility of the lipoplexes against free DNA (c), as a function of the cationic amphiphile/ DNA charge ratio. The red bars correspond to formulations in which the total positive charge is brought exclusively by SPYRIT-7 cationic lipid, while the green and violet bars represent SPYRIT-7/SPYRIT-68 blends of 95/5 and 90/10 charge contribution respectively. Error bars represent standard deviation (n = 10–12). P values were determined by one-way ANOVA, comparing the value with the previous one in the series ($^{\#}P < 0.05$, $^{\#\#}P < 0.01$, $^{\#\#\#}P < 0.001$ and $^{\#\#\#\#}P < 0.0001$). Only the statistical significant differences were shown.

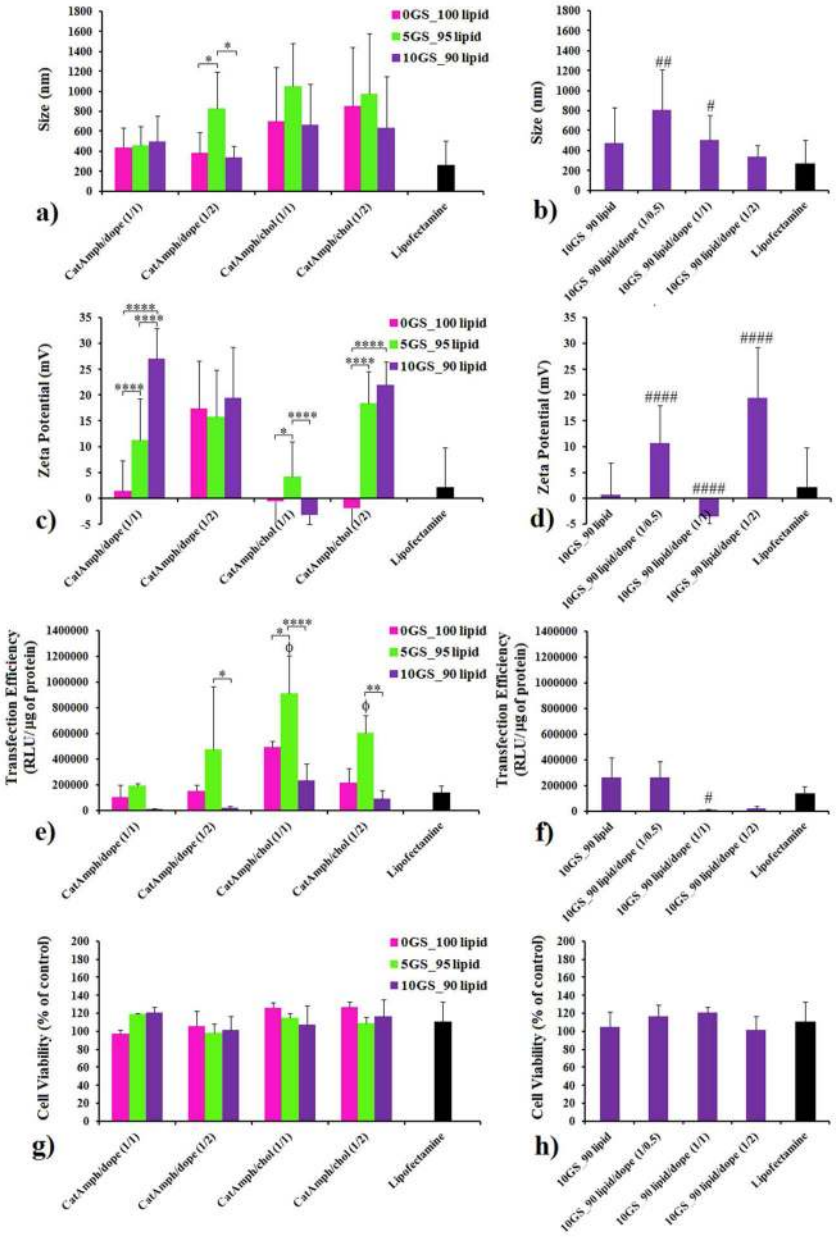

Figure 4.

Size (panels a, b), zeta potential (panels c, d), transfection efficiency (panels e, f) and cytotoxicity (panels g, h) against NCI-H23 cell line of lipoplexes formed at a +/− charge ratio of 3 from SPYRIT-68/SPYRIT-7 (0/100 red bars, 5/95 green bars, 10/90 violet bars) cationic amphiphiles coformulated with either DOPE or cholesterol at 1:1 and 1:2 molar ratios. P values were determined by two-way ANOVA within one set of formulations (*P < 0.05, **P < 0.01, ***P < 0.001 and ****P < 0.0001) or one-way ANOVA, comparing the value with the previous one ($^{\#}P$ <0.05, $^{\#\#}P$ < 0.01, $^{\#\#\#}P$ < 0.001 and $^{\#\#\#\#}P$ < 0.0001). In the transfection efficiency experiment (e, f) one-way ANOVA was performed relative to

Lipofectamine formulation ($^{\phi}P < 0.05$). Only the statistical significant differences were shown.

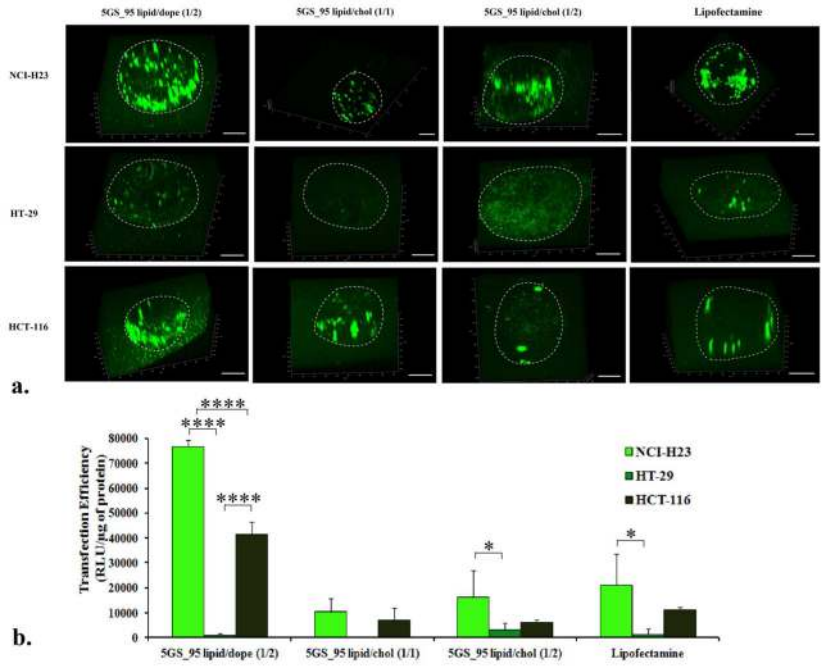

Figure 5.

Transfection of NCI-H23, HT-29, HCT-116 tumor spheroids by select pyridinium cationic amphiphiles formulations and commercial transfection reagent Lipofectamine®, as revealed by 3D images of GFP expression (a) and luciferase quantitation (b). Boundaries of spheroids are indicated by a dotted white line. Bar represents 200 μm. Note the strong cell dependence of transfection efficiency on cell type. P values were determined by two-way ANOVA within one set of formulations (*$P < 0.05$, **$P < 0.01$, ***$P < 0.001$ and ****$P < 0.0001$).

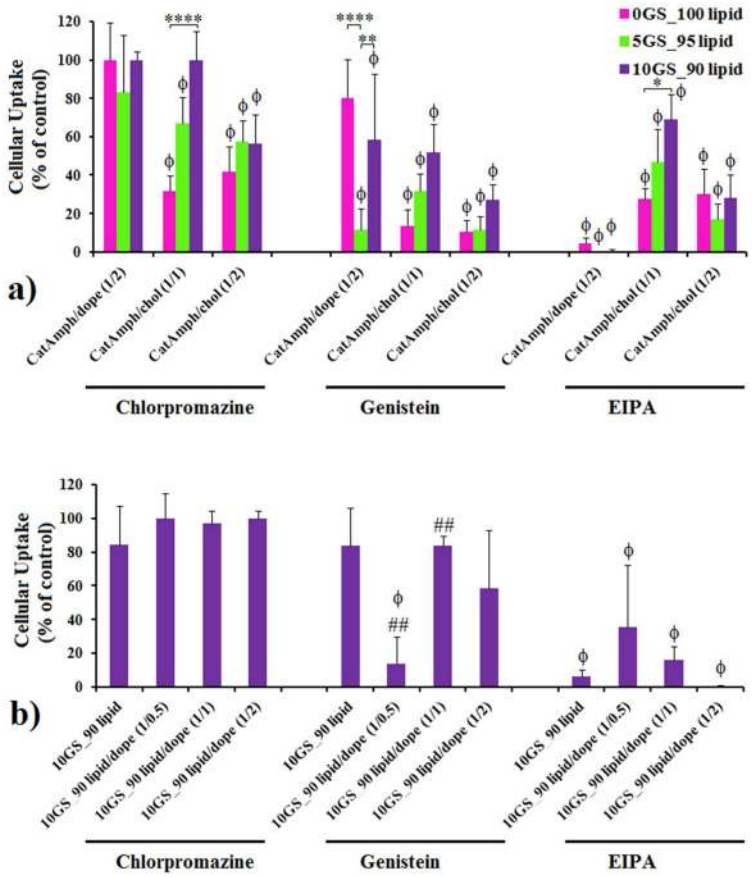

Figure 6.

Cellular uptake (NCI-H23 cell line) of lipoplexes formed from SPYRIT-7/SPYRIT-68 (0/100 red bars, 5/95 green bars, 10/90 violet bars) cationic amphiphiles coformulated with either DOPE or cholesterol at 1:1 and 1:2 molar ratios (a) or from SPYRIT-7/SPYRIT-68 (10/90) cationic amphiphiles formulated alone or with DOPE at different molar ratios (b) in the presence of specific internalization inhibitors chloropromazine, genistein and EIPA. P values were determined by one-way ANOVA, comparing the values with the control set ($^{\phi}P < 0.05$) in panels a) and b), by two-way ANOVA within one set of formulations ($^{*}P < 0.05$, $^{**}P < 0.01$, $^{***}P < 0.001$ and $^{****}P < 0.0001$) in panel a) and by one-way ANOVA, comparing the value within a series with the previous one ($^{\#}P < 0.05$, $^{\#\#}P < 0.01$, $^{\#\#\#}P < 0.001$ and $^{\#\#\#\#}P < 0.0001$) in panel b). Only the statistical significant differences were shown.

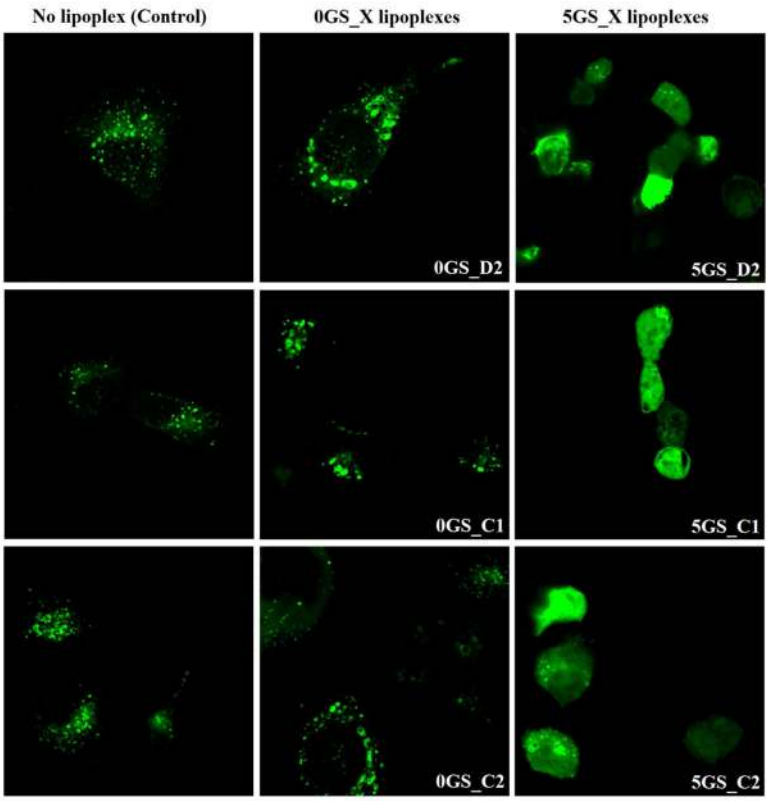

Figure 7.

Pyridinium GS promotes endolysosomal escape of the GS-containing lipoplexes: confocal images of NCI-H23 cells (excitation 488 nm) expressing the endolysosomal protein GFP-Rab 7 transfected with select lipoplex formulations indicated in each case; Rab-7 protein is specific for endolysosomes [57,58] as its specific distribution can be observed in control NCI-H23 cells that did not receive lipoplexes (left panels). Lipoplexes that do not contain GS do not change significantly Rab-7 intracellular distribution (central panels) while introduction of GS in the structure of lipoplexes promotes endolysosomal membrane rupture and consequently a diffuse distribution of Rab-7 in the cytoplasm, irrespective of the co-lipid used and its molar ratio in lipoplex formulations (right panels).

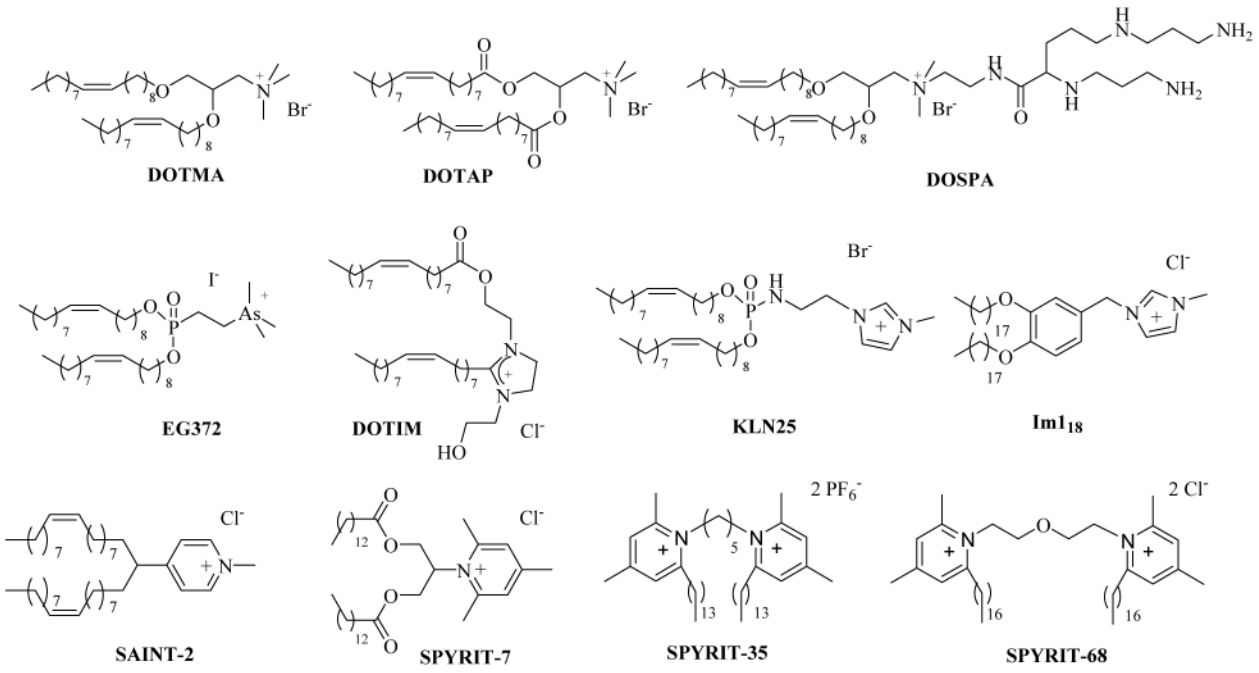

Chart 1.
Representative cationic lipids used in synthetic gene delivery systems